Micromagnetic simulations of current-induced magnetization switching in Co/Cu/Co nanopillars

Z. H. Xiao, X. Q. Ma,[a] and P. P. Wu
Department of Physics, University of Science and Technology Beijing, Beijing 100083, China

J. X. Zhang and L. Q. Chen
Department of Materials Science and Engineering, The Pennsylvania State University, University Park, Pennsylvania 16802, USA

S. Q. Shi
Department of Mechanical Engineering, The Hong Kong Polytechnic University, Hung Hom, Kowloon, Hong Kong

(Received 17 April 2007; accepted 31 August 2007; published online 6 November 2007)

We studied the current-induced magnetic switching in Co/Cu/Co nanopillars with an in-plane magnetization traversed by a perpendicular-to-plane spin-polarized current. The Landau-Lifshitz-Gilbert equation incorporating the spin transfer torque (STT) effect was employed. Magnetization switching was found to take place when the current density exceeds a threshold. It is accompanied by drastic oscillations near the magnetic reversal point. The switching time depends on the applied current density. The magnetization can also be switched by a sufficiently long square pulsed current. The roles of anisotropy, exchange, and demagnetization energies in the magnetization switching process of nanopillars are discussed. It is shown that the switching is mainly determined by the competition between STT and the Gilbert damping torque. © *2007 American Institute of Physics*. [DOI: 10.1063/1.2800999]

I. INTRODUCTION

When a spin-polarized current injected into a ferromagnetic thin film, a torque, called spin transfer torque (STT), is exerted on the local magnetic moments of a ferromagnet (FM). It is caused by the transfer of angular momentums from the electrons of the spin-polarized current to the ferromagnet. This mechanism was originally proposed by Berger[1] and Slonczewski[2] in 1996. Under sufficiently high current density, spin-wave excitations are stimulated, or the magnetization of a nanoscale magnetic film can be switched. The role of STT in magnetization switching has been verified by numerous experiments in spin-valve nanopillars,[3–10] magnetic nanowires,[11,12] point-contact geometry,[13–15] and magnetic tunnel junctions.[16–18] Compared with the conventional approach to switching magnetization using a magnetic field generated by an external current line, the applications of current-induced magnetization switching (CIMS) in a magnetic random access memory (MRAM) have the advantage of large storage density, high speed, low energy consumption, and avoidance of cross writing. Therefore, STT effect has been extensively studied by experiments, theories,[19–25] and numerical simulation studies.[26–32]

In the present work, we investigate the magnetization switching for a nanoscale pillar structure under the influence of a spin-polarized current through numerical simulations using the Landau-Lifshitz-Gilbert (LLG) equation incorporating STT effect. In particular, we studied the roles of magnetic anisotropy and demagnetization energy in the switching process.

II. MODEL DESCRIPTION

The nanopillar structure under investigation is schematically shown in Fig. 1. The thicknesses of each layer are Co(2 nm)/Cu(4 nm)/Co(10 nm) from top to bottom. The lateral size of the nanopillar is 64×64 nm^2. With two leads (not shown in Fig. 1) at 8 nm each, the size of the nanopillar is $32\times64\times64$ nm^3. The two Co layers (ferromagnets) are separated by a thin Cu layer (nonferromagnetic metal). The top Co layer is the free layer whose magnetization dynamics is triggered by a spin-polarized current. The bottom Co layer is the pinned layer with its magnetization vector **P** fixed in the direction along the positive x axis. As Co possesses uniaxial anisotropy, we assume that the easy axis of both Co layers is parallel to x axis. The free layer has two stable states, parallel or antiparallel to positive x axis. The initial magnetization vector **M** of the free layer is along the x axis.

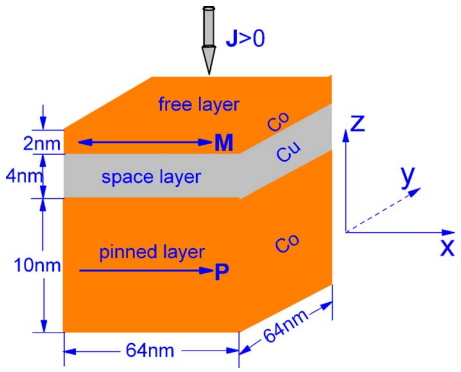

FIG. 1. (Color online) Model geometry definition of Co/Cu/Co nanopillar in Cartesian coordinates.

[a]Author to whom correspondence should be addressed. Electronic mail: xqma@sas.ustb.edu.cn

The middle Cu layer is a space layer whose function is to avoid the exchange coupling between the two Co layers. The electron current is spin polarized by the pinned layer and then passes through the space layer. The thickness of the space layer (4 nm) is much smaller than the spin diffusion length (approximately a few hundreds of nanometers) to conserve the spin momentum. We adopt the current-perpendicular-to-plane (CPP) geometry. The positive current is defined as the current flow from the free layer to the pinned layer and the conductive electrons flow in the opposite direction. Experimentally, the current-induced magnetization switching of antiferromagnetic coupling and uncoupling of Co/Cu/Co nanopillar structures have previously been investigated by Urazhdin *et al.*[33]

In our simulations, the entire nanopillar was divided into $16\times32\times32$ cubic grids with a grid size of $2\times2\times2$ nm^2. The magnetization within each grid is assumed to be uniform. The classical Oersted field generated by conduction electrons scales as $1/r$, where r is the lateral size of the free layer, while the STT scales as $1/r^2$. Therefore, for small r like a nanopillar, the STT dominates over the classical Oersted field. We ignore the Oersted field in this work.

The modified LLG equation[27] including the STT effect can be written as

$$\frac{d\mathbf{M}}{dt} = -\gamma'\mathbf{M}\times\mathbf{H}_{\text{eff}} - \frac{\alpha\gamma'}{M_s}\mathbf{M}\times(\mathbf{M}\times\mathbf{H}_{\text{eff}}) - \frac{2\mu_B J}{(1+\alpha^2)edM_s^3}g(\mathbf{M},\mathbf{P})\mathbf{M}\times(\mathbf{M}\times\mathbf{P}) + \frac{2\mu_B\alpha J}{(1+\alpha^2)edM_s^2}g(\mathbf{M},\mathbf{P})\mathbf{M}\times\mathbf{P}. \quad (1)$$

where $\mathbf{M}$ and $\mathbf{P}$ are the magnetization vectors of the free and pinned layers, respectively, $\gamma\prime=\gamma/(1+\alpha^2)$, γ is the gyromagnetic ratio, α is the dimensionless damping constant, $\mathbf{H}_{\text{eff}}$ is the effective field, M_s is the saturation magnetization of the free and pinned layers, μ_B is Bohr's magneton, J is the current density, d is the thickness of free layer, and e is the electron charge. The angle between $\mathbf{M}$ and $\mathbf{P}$ is θ, $\mathbf{M}\cdot\mathbf{P}/M_s^2=\cos\theta$. The scalar function $g(\mathbf{M},\mathbf{P})$ is given by[2]

$$g(\mathbf{M},\mathbf{P}) = [-4+(1+\eta)^3(3+\mathbf{M}\cdot\mathbf{P}/M_s^2)/4\eta^{3/2}]^{-1}, \quad (2)$$

where η is the spin polarizing factor. The first term in the modified LLG equation is the precession term that conserves the magnetic energy and determines the precession frequency of the magnetization dynamics. The second term is damping that dissipates the energy during magnetization. The last two terms describe the STT which tends to drag the magnetization away from its initial state to its final stable state and drives the magnetization precession around the effective field.

To initiate the simulation, a small angle deviation from the parallel or antiparallel configuration between $\mathbf{M}$ from $\mathbf{P}$ was assigned. The deviation can be understood as a result of thermal fluctuations. If $\mathbf{M}$ is parallel or antiparallel to $\mathbf{P}$ ($\theta=0°$ or $\theta=180°$), the STT is zero as $\mathbf{M}\times\mathbf{P}=0$. In our simulations, we assumed $\theta=0.1°$ for parallel and $\theta=179.9°$ for antiparallel configurations at the beginning.

We investigated the dynamics of magnetization by numerically solving the modified time-dependent LLG equation using the Gauss-Seidel projection method[34,35] with a constant time step $\Delta t=0.014\,875$ ps. $\mathbf{H}_{\text{eff}}$ can be represented as a variational derivative of the energy E of the system with respect to magnetization

$$\mathbf{H}_{\text{eff}} = -\frac{1}{\mu_0}\frac{\delta E}{\delta\mathbf{M}}, \quad (3)$$

where μ_0 is the permeability of vacuum. The total energy E is given by

$$E = E_{\text{ani}} + E_{\text{exch}} + E_{\text{ms}} + E_{\text{ext}}, \quad (4)$$

where E_{ani} denotes the anisotropy energy, E_{exch} the exchange energy, E_{ms} the magnetostatic energy, and E_{ext} the Zeeman energy. The energy of the STT was not included in Eq. (4) and considered separately.

The anisotropy energy of Co in a Co/Cu/Co nanopillar is

$$E_{\text{ani}} = \int (K_1[1-m_x^2(r)] + K_2\{[1-m_x^2(r)]\}^2)d^3r, \quad (5)$$

where K_1 and K_2 are the anisotropy constants, $m_x(r)$ is the unit magnetization vector at each grid, $m_x(r)=M_x(r)/M_s$, and the easy axis is along the x axis. Considering the fact that K_1 is far greater than K_2, we ignore the second term in the simulations.

The exchange energy is

$$E_{\text{exch}} = \int \left(\frac{A}{M_s^2}|\nabla\mathbf{M}(\mathbf{r})|^2\right)d^3r, \quad (6)$$

where A is the exchange stiffness constant.

The magnetostatic energy can be presented as a sum of energies of interacting magnetic dipoles as follows:

$$E_{\text{ms}} = \frac{1}{2}\int\int\left\{M_i(\mathbf{r})\left[\frac{\delta_{ij}}{|\mathbf{r}-\mathbf{r}'|^3} - \frac{3(r_i-r_i')(r_j-r_j')}{|\mathbf{r}-\mathbf{r}'|^5}\right]M_j(\mathbf{r})\right\}d^3r d^3r'. \quad (7)$$

We utilize the fast Fourier transform (FFT) technique for obtaining the magnetostatic energy as it involves double integrals in real space.[35]

The Zeeman energy is

$$E_{\text{ext}} = -\mu_0\int[\mathbf{H}_{\text{ext}}\cdot\mathbf{M}(\mathbf{r})]d^3r, \quad (8)$$

where $\mathbf{H}_{\text{ext}}$ is the externally applied magnetic field.

The energy of the STT is

$$E_{\text{STT}} = -\mu_0\int[\mathbf{H}_{\text{STR}}\cdot\mathbf{M}(\mathbf{r})]d^3r, \quad (9)$$

where $\mathbf{H}_{\text{STT}}$ is the corresponding effective field given by

$$\mathbf{H}_{\text{STT}} = 2\mu_B J g(\mathbf{M},\mathbf{P})\mathbf{M}\times\mathbf{P}/(\gamma edM_s^3). \quad (10)$$

In our simulations, we adopted the properties of Co at helium temperature (4.2 K): $\eta=0.35$, $M_s=1.446\times10^6$ A/m, $\gamma=2.3245\times10^5$ m/(A s), $\alpha=0.01$, $K_1=6.86\times10^5$ J/m^3,[36]

$A=2.0\times10^{-11}$ J/m, and $d=2$ nm. Our focus is on the cases that the two Co layers have negligible antiferromagnetic coupling in a Co/Cu/Co nanopillar.

III. RESULTS AND DISCUSSIONS

We will first discuss the magnetization switching of nanopillars by incorporating all the energetic contributions including the energy of STT, anisotropy, demagnetization, exchange, and Gilbert damping. We will then examine the importance of the anisotropy and demagnetization energies, respectively, by deliberately removing one or both of them in the magnetization switching process (Sec. III A). In Sec. III B, we will define the switching time and discuss the magnetization switching process under constant or square pulsed electrical currents. The relationship between switching time and current density will be discussed.

A. Magnetization switching and the role of anisotropy and demagnetization energy in switching

Our simulations show that the magnetization can flip from an initial parallel state (PS) to a final antiparallel state (APS) when the current density flow from the pinned layer to the free layer exceeds $J_c^{\mathrm{PS}\rightarrow\mathrm{APS}}=-1.4\times10^8$ A/cm^2 (PS$\rightarrow$APS) under zero external field. The reversal process was realized when a reversal current density over $J_c^{\mathrm{APS}\rightarrow\mathrm{PS}}=6.0\times10^7$ A/cm^2 (APS$\rightarrow$PS) was applied. It is quite remarkable that without explicitly fitting to experimental measurements, our predicted threshold current density shows an excellent agreement with experimentally measured values[4,5,9] ranging from 10^7 to 10^8 A/cm^2. A positive current density favors the parallel alignment while a negative one leads to an antiparallel configuration. The magnetization switching is mainly determined by the competition of spin transfer and Gilbert damping torques. The magnetization can be switched only when STT is greater than the Gilbert damping torque. The STT is proportional to the current density. The higher the current density, the higher the STT is. The Gilbert damping torque is proportional to the effective field $[\alpha\gamma'\mathbf{M}\times(\mathbf{M}\times\mathbf{H}_{\mathrm{eff}})/M_s]$. The effective field consists mainly of contributions from anisotropy, demagnetization, and exchange energies. Therefore, the value of the threshold current density was influenced by a number of factors including the anisotropy constant, exchange stiffness, Gilbert damping parameter, the saturation magnetization, and the thickness of the free layer. In Fig. 2, we show the temporal evolution of the three components of magnetization in the free layer under the constant current density of -1.4×10^8 A/cm^2 (a) and the reversal process under the constant current density of 6.0×10^7 A/cm^2 (b).

As shown in Fig. 2, switching is accompanied by drastic oscillations which are the result of the magnetization precession around the effective field in the switching process. $\mathbf{m}=\mathbf{M}/M_s$. $\langle M_x\rangle$, $\langle M_y\rangle$, and $\langle M_z\rangle$ are averages over the free layer. In fact, as soon as the current was applied, the magnetization oscillation occurs until the final static state is reached. It is maximal near the reversal transition. The oscillations for the y and z components of magnetization are more dramatic than the x component. The temporal evolution of

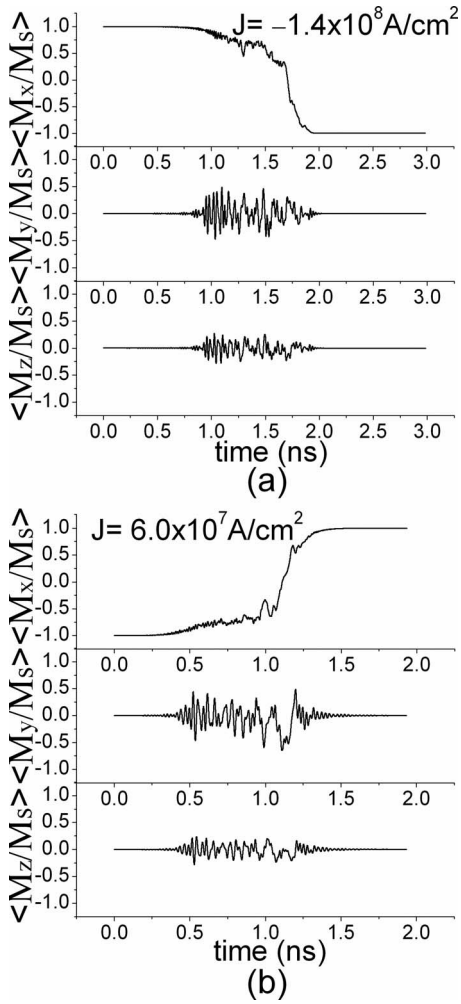

FIG. 2. The temporal evolution of M_x, M_y, and M_z under the spin-polarized current during the switching process. (a) PS$\rightarrow$APS at the threshold current density of -1.4×10^8 A/cm^2, and (b) APS$\rightarrow$PS at 6.0×10^7 A/cm^2.

M_y is similar to M_z although the maximal magnitude of M_y is greater than that of M_z. The difference between M_y and M_z originates from the demagnetization energy as a result of different thicknesses along the y and z directions of the free layer.

The threshold current density for PS$\rightarrow$APS is very different from APS$\rightarrow$PS: $\Delta J_c=|J_c^{\mathrm{PS}\rightarrow\mathrm{APS}}|-|J_c^{\mathrm{APS}\rightarrow\mathrm{PS}}|=8.0\times10^7$ A/cm^2, or $\Delta J_c/d=4.0\times10^7$ A/(cm^2 nm). Similar difference has been observed experimentally with a value of $(3.2\pm0.2)\times10^7$ A/(cm^2 nm) for Co/Cu/Co nanopillars.[6] In our simulations, we adopted Slonczewski's model, which only takes into account the interface spin-flip scattering between the layers. The relationship between STT and θ in Slonczewski's model is plotted in Fig. 3.

$\mathbf{H}_{\mathrm{STT}}$ is the effective field from the STT for current density of 2.0×10^8 A/cm^2 described by Eq. (10), and θ is the angle between the magnetization of the free layer ($\mathbf{M}$) and the pinned layer ($\mathbf{P}$). The STT is maximum at $\theta=127.17°$, which makes the switching easier from the antiparallel to the parallel state (APS$\rightarrow$PS) than from parallel to the antiparallel state (PS$\rightarrow$APS). This explains the fact that $|J_c^{\mathrm{APS}\rightarrow\mathrm{PS}}|$ is far lower than $|J_c^{\mathrm{PS}\rightarrow\mathrm{APS}}|$.

To study the role of magnetic anisotropy and demagnetization energy, we simulated the switching dynamics with

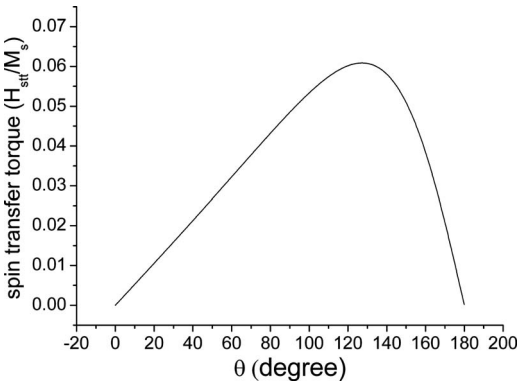

FIG. 3. The relationship of STT vs θ of Slonczewski's model.

the anisotropy energy E_{ani} or demagnetization energy E_{dem} or both removed. The temporal evolution of all three components without taking into account the anisotropy energy is shown in Fig. 4(a). During the switching process, the z component of magnetization, M_z, is almost always zero, and hence the magnetization switching activities only take place on the x-y plane. This originates from the fact that the size of the free layer in x direction is equal to that of y direction (both are 64 nm) and significantly larger than z direction (2 nm), and thus a much lower demagnetization energy along x and y directions than the z direction. The higher demagnetization energy E_{dem} of z direction impedes the development of the z component. Therefore, without anisotropy energy E_{ani}, the demagnetization energy E_{dem} has a great influence on the magnetization dynamics.

Figure 4(b) shows the evolution dynamics of the three magnetization components without taking into account the demagnetization energy. The magnetizations M_y and M_z oscillate, and their amplitudes reach maximum in the transition regime towards reversal. There is no oscillation occurred at the x component of magnetization in this situation. As we mentioned above, the oscillation of M_x and the difference between the maximal oscillation amplitudes of M_y and M_z are the consequences of the demagnetization energy. In this case, the effective field mainly consists of the anisotropy field whose direction is along the x axis in the switching process, and the magnetization switches with precession around the x axis by the effective field, leading to oscillations in M_y and M_z.

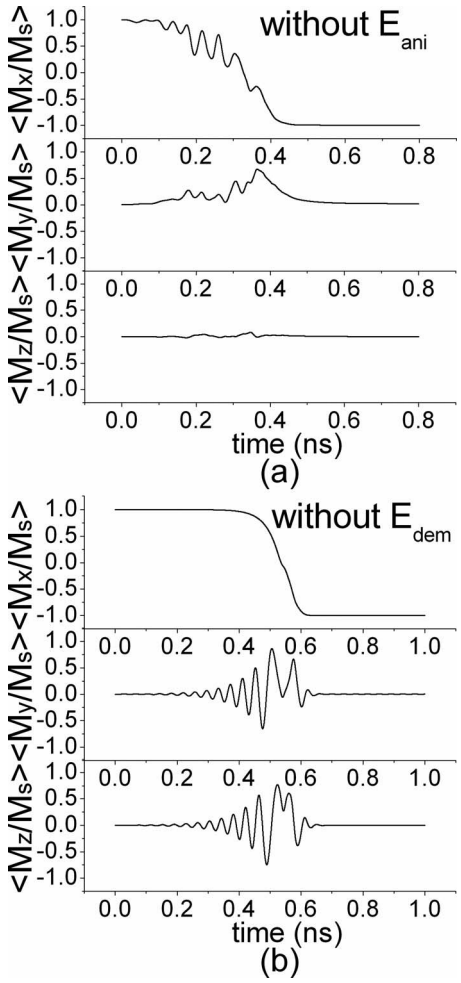

FIG. 4. Temporal evolution of magnetization. (a) is the temporal evolution of three components of magnetization (PS→APS) under the negative constant current density of -3.0×10^8 A/cm^2 without taking into account anisotropy energy E_{ani}. (b) is the temporal evolution of three components of magnetization (PS→APS) under the negative constant current density of -3.0×10^8 A/cm^2 without taking into account demagnetization energy E_{dem}.

B. Switching time

Switching of magnetization not only requires sufficiently high current density but also sufficiently long current application time. For a given current density above a threshold value, there is a unique switching time. In Fig. 5, we show the temporal evolution of M_x under square pulsed and constant electrical currents. The minimum pulse width needed to switch the magnetization is defined as the switching time t_s. For the sake of convenience, both square pulsed current and constant current are applied at $t=0$.

Figure 5 clearly demonstrates that there is a minimum switching time for a given current. The two cases, constant and pulse currents, show differences in the switching behavior [the second and third graphs of (a) and (b) in Fig. 5]. For the case of a pulse current, there is no STT in the final stage of switching while for the case of constant current, the STT exists through the whole magnetization switching process. The magnetization approaches the final state faster in the presence of a STT.

The anisotropy and demagnetization energies have a large influence on the switching time. As we mentioned it above, the anisotropy and demagnetization energies influence the switching indirectly through the Gilbert damping torque. Therefore, they affect the switching time indirectly. The anisotropy energy impedes switching and thus increases the switching time. On the other hand, the demagnetization energy favors switching. When both the anisotropy and demagnetization energies are taken into account, the switching time is extended. In the PS→APS switching process, the direction of anisotropy field is along the positive x axis before switching, so the Gilbert damping torque offsets most parts of the STT, and thus extends the switching time. The Gilbert damping torque induced by the demagnetization field favors the magnetization direction along the diagonal of x-y plane, and thus promotes the switching of magnetization

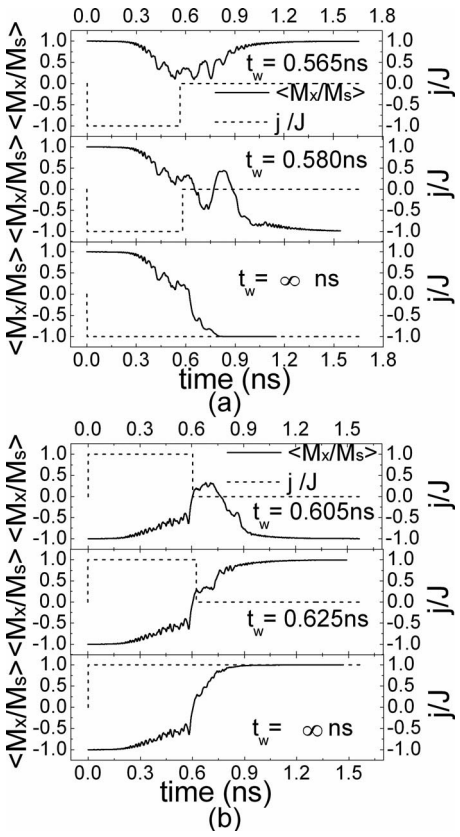

FIG. 5. The temporal evolution of M_x under square pulsed and constant currents. For (a) $J=3.0\times10^8$ A/cm^2 (PS→APS) and for (b) $J=0.9\times10^8$ A/cm^2 (APS→PS). Current density j (dash line) is plotted as a function of time. J is the maximum of j. t_w is the impulse width.

from $+x$ axis to the x-y diagonal, which drastically reduces the switching time. The effects of magnetic anisotropy and demagnetization on the APS→PS switching are similar to PS→APS. Switching time is extended due to oscillations in M_x under the influence of magnetic anisotropy and demagnetization.

It should be noted that the exchange energy may have an influence on switching when the free layer is not a single domain. This is true in the vicinity of the transition point during switching when the current density is close to the threshold current density. The presence of multidomain in the switching process will increase the switching time.

As expected, increasing the current density shortens the switching time. Figure 6 shows the switching time as a function of applied current density J_c, indicating an approximate inverse relationship. The switching time is the largest at the threshold current density of 6.0×10^7 A/cm^2 for APS→PS and -1.4×10^8 A/cm^2 for PS→APS. As the absolute current density increases, the switching time approaches a small value asymptotically. Therefore, the efficiency of reducing switching time through increasing absolute current density is not salient when the absolute current density exceeds about 3.0×10^8 A/cm^2 for APS→PS and 4.0×10^8 A/cm^2 for PS→APS. As one can see from Fig. 6, switching time is typically on the order of nanoseconds, consistent with the experimental values in Co/Cu/Co nanopillars.[37] The predicted relationships between applied current density and switching time can potentially provide guidance for designing MRAM devices.

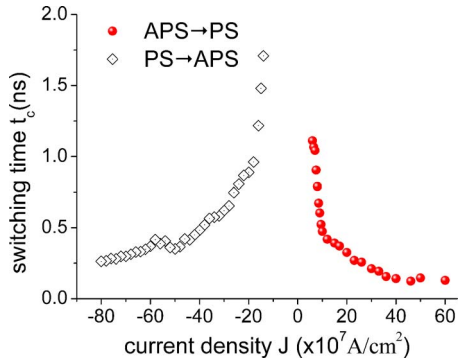

FIG. 6. (Color online) The relationship of switching time t_s vs the current density J_c.

In summary, magnetization dynamics in the presence of a STT is modeled. Magnetization switching is mainly determined by the competition between the STT and the Gilbert damping torque. It is found that while the spin-polarized current is the dominant driving force for switching, other contributions such as magnetic anisotropy and demagnetization energy also play important roles. Our predicted values of critical current density and switching times are in very good agreement with existing experimental measurements. It is shown that the switching time versus the applied current density is close to an inverse relation.

ACKNOWLEDGMENTS

This work was sponsored by the Joint Research Fund for Overseas Chinese Young Scholars from the National Science Foundation of China (5042810) and by SRF for ROCS, SEM.

[1] L. Berger, Phys. Rev. B **54**, 9353 (1996).
[2] J. C. Slonczewski, J. Magn. Magn. Mater. **159**, L1 (1996).
[3] E. B. Myers, D. C. Ralph, J. A. Katine, R. N. Louie, and R. A. Buhrman, Science **285**, 867 (1999).
[4] J. Grollier, V. Cros, A. Hamzic, J. M. George, H. Jaffres, A. Fert, G. Faini, J. Ben Youssef, and H. Legall, Appl. Phys. Lett. **78**, 3663 (2001).
[5] J. A. Katine, F. J. Albert, R. A. Buhrman, E. B. Myers, and D. C. Ralph, Phys. Rev. Lett. **84**, 3149 (2000).
[6] F. J. Albert, N. C. Emley, E. B. Myers, D. C. Ralph, and R. A. Buhrman, Phys. Rev. Lett. **89**, 226802 (2002).
[7] J. Z. Sun, D. J. Monsma, M. J. Rooks, and R. H. Koch, Appl. Phys. Lett. **81**, 2202 (2002).
[8] S. I. Kiselev, J. C. Sankey, I. N. Krivorotov, N. C. Emley, R. J. Schoelkopf, R. A. Buhrman, and D. C. Ralph, Nature (London) **425**, 380 (2003).
[9] B. Özyilmaz, A. D. Kent, D. Monsma, J. Z. Sun, M. J. Rooks, and R. H. Koch, Phys. Rev. Lett. **91**, 067203 (2003).
[10] S. Urazhdin, N. O. Birge, W. P. Pratt, and J. Bass, Phys. Rev. Lett. **91**, 146803 (2003).
[11] J. E. Wegrowe, X. Hoffer, Ph. Guittienne, A. Fabian, L. Gravier, T. Wade, and J. Ph. Ansermet, J. Appl. Phys. **91**, 6806 (2002).
[12] D. Kelly, J.-E. Wegrowe, T.-K. Truong, X. Hoffer, P. Guittienne, and J.-P. Ansermet, Phys. Rev. B **68**, 134425 (2003).
[13] M. Tsoi, A. G. M. Jansen, J. Bass, W.-C. Chiang, M. Seck, V. Tsoi, and P. Wyder, Phys. Rev. Lett. **80**, 4281 (1998).
[14] W. H. Rippard, M. R. Pufall, S. Kaka, S. E. Russek, and T. J. Silva, Phys. Rev. Lett. **92**, 027201 (2004).
[15] T. Y. Chen, Y. Ji, C. L. Chien, and M. D. Stiles, Phys. Rev. Lett. **93**, 026601 (2004).
[16] J. Z. Sun, J. Magn. Magn. Mater. **202**, 157 (1999).

[17]Y. Liu, Z. Zhang, P. P. Freitas, and J. L. Martins, Appl. Phys. Lett. **82**, 2871 (2003).
[18]Y. Huai, M. Pakala, Z. Diao, and Y. Ding, Appl. Phys. Lett. **87**, 222510 (2005).
[19]Y. B. Bazaliy, B. A. Jones, and S.-C. Zhang, Phys. Rev. B **57**, R3213 (1998).
[20]J. C. Slonczewski, J. Magn. Magn. Mater. **195**, L261 (1999).
[21]J. Z. Sun, Phys. Rev. B **62**, 570 (2000).
[22]C. Heide, P. E. Zilberman, and R. J. Elliott, Phys. Rev. B **63**, 064424 (2001).
[23]M. D. Stiles and A. Zangwill, J. Appl. Phys. **91**, 6812 (2002); Phys. Rev. B **66**, 014407 (2002).
[24]S. Zhang, P. M. Levy, and A. Fert, Phys. Rev. Lett. **88**, 236601 (2002).
[25]A. Shpiro, P. M. Levy, and S. Zhang, Phys. Rev. B **67**, 104430 (2003).
[26]Z. Li and S. Zhang, Phys. Rev. B **68**, 024404 (2003).
[27]L. Torres, L. Lopez-Diaz, E. Martinez, M. Carpentieri, and G. Finocchio, J. Magn. Magn. Mater. **286**, 381 (2005).
[28]M. Carpentieri, G. Finocchio, B. Azzerboni, L. Torres, L. Lopez-Diaz, and E. Martinez, K. J. Lee, O. Redon, and B. Dieny, Appl. Phys. Lett. **86**, 022505 (2005).
[29]T. Devolder, P. Crozat, C. Chappert, J. Miltat, A. Tulapurkar, Y. Suzuki, K. Yagami, Z. Li, and S. Zhang, Phys. Rev. B **71**, 184401 (2005).
[30]H. Xi, Y. Shi, and K.-Z. Gao, Phys. Rev. B **71**, 144418 (2005).
[31]D. V. Berkov and N. L. Gorn, Phys. Rev. B **72**, 094401 (2005).
[32]Y. Zhang, Z. Zhang, Y. Liu, B. Ma, and Q. Y. Jin, J. Appl. Phys. **99**, 08G515 (2006).
[33]S. Urazhdin, H. Kurt, W. P. Pratt, Jr., and J. Bass, Appl. Phys. Lett. **83**, 114 (2003).
[34]X. P. Wang, C. J. Garcia-Cervera, and E. Weinan, J. Comput. Phys. **171**, 357 (2001).
[35]J. X. Zhang and L. Q. Chen, Acta Mater. **53**, 2845 (2005); J. Appl. Phys. **97**, 084313 (2005).
[36]S. Chikazumi, T. Wakiyama, and K. Yosida, Proceedings of the International Conference on Magnetism Nottingham, 1964 (unpublished), p. 756.
[37]M. R. Pufall, W. H. Rippard, S. Kaka, S. E. Russek, T. J. Silva, J. Katine, and M. Carey, Phys. Rev. B **69**, 214409 (2004).